# Copper-related deep-level centers in irradiated *p*-type silicon

Nikolai Yarykin*
*Institute of Microelectronics Technology RAS, 142432 Chernogolovka, Russia*

Jörg Weber
*Technische Universität Dresden, D-01062 Dresden, Germany*
(Received 21 December 2010; published 28 March 2011)

Deep-level centers are investigated in the *p*-type Si on copper-contaminated samples which were also electron irradiated. Standard and Laplace-transform deep-level transient spectroscopy techniques were employed to characterize the samples. Several Cu-related centers are observed to form either as a result of the low-temperature Cu diffusion into the irradiated crystals or due to irradiation of the Cu-contaminated samples and subsequent annealing up to 400 °C. In all crystals, two Cu-related defects are found to be the most abundant; each of them possesses a pair of levels in the lower half of the gap. The Arrhenius signatures for one pair are measured to be practically identical to those for the donor and acceptor levels of substitutional copper $Cu_s$, respectively, the levels of other defect being only barely different from the $Cu_s$ levels. Analysis of the introduction rates and depth profiles of the deep-level centers points to the vacancy–oxygen complex (VO, the A center) as the precursor of the most abundant Cu-related defects. It is inferred that $Cu_s$ is formed in irradiated silicon due to interaction with the VO centers via the rather stable intermediate CuVO complex.

DOI: 10.1103/PhysRevB.83.125207 PACS number(s): 61.72.J−, 61.82.Fk, 71.55.Cn

## I. INTRODUCTION

Copper exhibits in Si properties which are significantly different from those of other 3*d* transition metals. Copper is also of practical importance as (i) it is used for the interconnections on silicon chips, (ii) easily contaminates the crystal bulk, and (iii) tends to form electrically active precipitates which degrade the function of devices. However, despite numerous investigations (for reviews, see Refs. 1–4), our knowledge about copper-related defects in silicon is still incomplete. In particular, only a few studies dealt with the interactions of copper with radiation defects which are unintentionally formed during many technological processes. The study of copper interaction with radiation-induced defects might lead to a better understanding of the nucleation sites for copper precipitation.

All experimental data on the electrically active centers in the irradiated Cu-contaminated silicon were obtained using the deep-level transient spectroscopy (DLTS) technique. In *n*-type crystals, the presence of Cu leads to a significant drop in the annealing temperatures at which dominant radiation defects, the A centers (VO) and divacancies ($V_2$), disappear from the DLTS spectra.[5,6] The effect is attributed to a decoration of the radiation defects with the mobile Cu atoms, which leads to a change in their electrical activity. The enhanced annealing leads to the formation of two new deep levels at $E_c - 0.17$ and $E_c - 0.60$ eV ($E_c$ is the bottom of the conduction band) which were tentatively ascribed to the $CuV_2$ and CuVO complexes, respectively.[6]

The Cu impact on the DLTS spectrum of irradiated *p*-type Si was reported previously.[7,8] After $\gamma$-irradiation of the Cu-contaminated samples, Pearton and Taveldale[7] did not detect any new radiation defects with levels in the lower half of the gap. Aboelfotoh and Svensson introduced copper into already irradiated crystals from copper Schottky barriers.[8] The reported results are, in general, similar to those in *n*-type crystals. The dominant radiation defects, the divacancies and $C_iO_i$ pairs, anneal out at 100–150 °C, which is much lower than without copper contamination. The interaction of copper and radiation defects results in the formation of a new center with a level at $E_v + 0.52$ eV ($E_v$ stands for the top of the valence band). It was suggested that the new center is a complex of Cu and the $C_iO_i$ pair.[8] However, this identification has been ruled out recently,[9] which leaves the nature of the center unknown.

In this paper we present an extended study on the interaction of copper with radiation defects in *p*-type silicon and concentrate, in particular, on the nature of doping impurity, thermal stability of the Cu-related deep-level (DL) centers, and the precursors of the Cu-related radiation defects. Some preliminary results of this study have been published already in Ref. 9.

## II. EXPERIMENT

### A. Crystals and irradiation

Six different *p*-type silicon crystals doped either with boron or gallium have been used in our study (see Table I). From the intensity of the 1106 $cm^{-1}$ IR absorption line at 300 K, the oxygen concentration in all Cz-grown crystals was determined in the range of (0.7–1.0) $\times 10^{18}$ $cm^{-3}$. The substitutional carbon concentration was below the detection limit ($\sim 4 \times 10^{16}$ $cm^{-3}$) in all samples.

Radiation defects were introduced by the exposure of the samples to electrons with an average energy of ∼5 MeV and a flux of $\sim 5 \times 10^{11}$ $cm^{-2}$ $s^{-1}$. The irradiation dose $\Phi$ was adjusted in the range of (0.7–10) $\times 10^{15}$ $cm^{-2}$ to keep concentrations of the most abundant DL centers at a level 5–15% of the doping level. To prevent heating under the electron beam the wafers were mounted on a water-cooled metal block. A part of the irradiated samples was kept in a refrigerator at ∼−15 °C until the handling before the measurements.

 ©2011 American Physical Society

TABLE I. Growth method and shallow-acceptor doping of the samples used in the study.

| Crystal no. | Growth method[a] | Shallow acceptor | Concentration ($10^{15}$ cm$^{-3}$) |
|---|---|---|---|
| 1 | Cz | B | 1.2 |
| 2 | Cz | B | 0.8 |
| 3 | Cz | Ga | 1.8 |
| 4 | FZ | Ga | 0.6 |
| 5 | FZ | B | 14 |
| 6 | Cz | B | 6.5 |

[a]Cz and FZ stand for crystals grown by the Czochralski or floating-zone methods, respectively.

### B. Copper introduction

Two different approaches were used to investigate the interaction of copper with radiation defects. They are (i) a high-temperature Cu diffusion into the initial crystals (HT-Cu diffusion) with subsequent electron irradiation and thermal annealing and (ii) a low-temperature Cu incorporation (LT-Cu treatment) into already irradiated (and thermally annealed) samples.

The HT-Cu diffusion was performed in Cu-contaminated quartz ampoules at 750 °C for 20 min and terminated by quenching into liquid nitrogen. Taking into account the Cu diffusivity,[3] the thermal budget is enough to ensure a homogeneous Cu distribution in the wafers. At 750 °C the Cu solubility in silicon exceeds $10^{16}$ cm$^{-3}$.[1] Because the ampoules were not sealed but had a cold open end, the final Cu concentration is below the saturation limit and depends on the extent of Cu contamination of the ampoule.

After diffusion at 750 °C, copper is expected to be mainly in the form of interstitial positively charged $Cu_i^+$ ions and Cu-acceptor complexes.[3,4] Since the $Cu_i^+$ diffusivity is high[10] and the binding energies of the Cu-acceptor pairs are small,[11,12] all copper remains rather mobile at room temperature ($D_{eff} > 10^{-9}$ cm$^2$ s$^{-1}$ in all wafers). Therefore, the HT-Cu diffused samples were kept in a refrigerator at ∼−15 °C until subsequent irradiation and measurements.

To evaluate the amount of Cu, the Schottky diodes made on the HT-Cu diffused samples were cooled down from room temperature under constant reverse bias, which resulted in the removal of copper from the near-surface region. The capacitance-voltage ($CV$) measurements at 200 K reveal a step in the depth profiles of the net acceptor concentration, with a step amplitude equal to the Cu concentration.[12] The amount of copper determined by this method in our HT samples was in the range of ∼ (0.5–10) × $10^{14}$ cm$^{-3}$. The DLTS measurements reveal that concentration of the $E_v + 0.1$ eV level, which is often observed in the Cu-doped Si,[13,14] does not exceed $10^{13}$ cm$^{-3}$ in the samples with the highest Cu contamination. No other deep levels are present with concentrations above $10^{12}$ cm$^{-3}$ in the nonirradiated HT-Cu diffused wafers.

The LT-Cu treatment was performed in two steps. First, samples were subjected to a chemical etching for 2 min in the Cu-contaminated acid solution ($HF:HNO_3 = 1:7$, 100 mg of Cu per 100 ml of the solution) which was terminated with a rinse in water. Then, the etched samples were annealed at 350 K for 3 h in air. After the LT-Cu treatment of the initial (nonirradiated) crystals, the DL concentration was below $10^{11}$ cm$^{-3}$. The annealing of irradiated samples at 350 K after the etching in an uncontaminated etch solution results in no significant variations of the DLTS spectrum except those which are known to occur due to hydrogen penetration.[15,16]

The effective Cu diffusivity at room temperature is about $10^{-7}$ cm$^2$/s in silicon doped with boron to an ∼$10^{15}$ cm$^{-3}$ level.[10] Therefore, copper deposited from the contaminated solution could penetrate about 100 $\mu$m into the bulk already during the sample handling (∼20 min). However, no copper-related defect is observed without the thermal stimulation at 350 K. Most likely, this indicates that copper is captured at (or close to) the surface and is released from there by the additional heating.

### C. Measurements

For the electrical measurements Schottky diodes were prepared by thermal Al evaporation through metal masks with holes of 1–2 mm diameter, depending on the sample doping level. Immediately prior to the evaporation the samples were chemically etched in an acid solution ($HF:HNO_3:CH_3COOH = 1:2:1$) to remove ∼30 $\mu$m from the surface. The etching was omitted after the LT-Cu treatment (see Sec. II B). In this case only a rinse in 10% HF solution was applied. Ohmic contacts were formed by rubbing a eutectic InGa alloy onto the back side of the samples.

Standard DLTS measurements were performed in the temperature range 35–340 K with a modified Boonton 72B capacitance meter and a lock-in amplifier with the sine correlation function. Typically, the filling pulse duration and the setup rate window were set to 1 ms and 49 s$^{-1}$, respectively. For presentation of the deep-level spectra throughout the paper, the raw DLTS signals ($\Delta C$) were multiplied by a factor $V_r/(V_r - V_p)$, where $V_r$ and $V_p$ are the reverse bias and filling pulse voltages, respectively, to ensure that the defects with equal concentrations provide the peaks of approximately the same amplitude.

The spatial distributions of DL centers were calculated from dependence of the DLTS signal on the filling pulse amplitude at a fixed reverse bias. The inhomogeneous profiles of shallow dopants, which were determined from the $CV$ measurements, and the so-called transition region[17] (or $\lambda$ layer[18]) were properly included in the calculations.

The Laplace-DLTS technique (LDLTS)[19] was applied to resolve overlapping DLTS peaks and to determine precisely activation energies. The LDLTS setup was operated in the temperature range 80–300 K under control of the Laplace transient processing system (version 3.2).

## III. RESULTS AND DISCUSSION

### A. Cu introduction into irradiated samples

The effect of the LT-Cu treatment (see Sec. II B) on the DL spectrum of the electron-irradiated crystals is shown in Fig. 1. The dashed curves represent a typical DLTS spectrum for pure (no copper) $p$-type irradiated samples, which consists primarily of two peaks: the donor levels of the divacancy and the $C_iO_i$ pair. The introduction of copper at 350 K results in the appearance of several additional features (solid curves

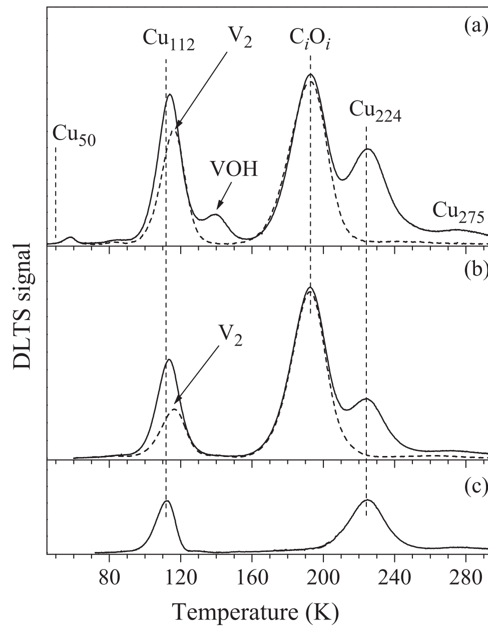


FIG. 1. (a) and (b) DLTS spectra of the electron-irradiated Si crystals before (dashed curves) and after (solid curves) the LT-Cu treatment at 350 K. (a) Boron-doped crystal no. 1 (see Table I), irradiation dose $\Phi = 7 \times 10^{14}$ cm$^{-2}$; (b) gallium-doped crystal no. 3, $\Phi = 3 \times 10^{15}$ cm$^{-2}$. All spectra were taken from the depth of 1–2 $\mu$m. The rate window was set to 49 s$^{-1}$. The spectrum (c) is calculated as the difference of the two curves in plot (b).

in Fig. 1). Peaks $Cu_{112}$, $Cu_{224}$,[20] and $Cu_{275}$ are distinct for copper contamination of the samples. (In the $Cu_{xxx}$ notation the subscript indicates the temperature at which the peak maximum occurs under standard measurement conditions, i.e., a rate window of 49 s$^{-1}$ in our case.) The VOH center is formed due to hydrogen penetration from the etched surface during the annealing.[15]

The position of the prominent $Cu_{224}$ peak is very similar to that which was reported in samples where copper was interacting with radiation defects at near room temperature.[8] The Cu-related nature of the $Cu_{275}$ level has been established by the constant [$Cu_{275}$]/[$Cu_{224}$] ratio (brackets indicate the concentration value) in the samples with different Cu concentrations.[9] As for the $Cu_{112}$ feature, the nature of this level has not been discussed earlier. The vertical line denoted as $Cu_{50}$ in Fig. 1(a) indicates the expected position of the Cu-related $E_v + 0.1$ eV level.[13,14] This level was never detected in our LT-Cu treated samples. The small peak of unknown nature at 58 K observed in many irradiated Si crystals is not related to copper.

The LT-Cu treatment of the gallium-doped material forms the same Cu-related levels with similar relative amplitudes [Fig. 1(b)]. Thus, shallow acceptors appear not to be constituents of the observed Cu-related centers. However, the Ga-doped crystals offer some advantages over the boron-doped ones in the study of Cu-related defects as will be discussed below.

### B. $Cu_{112}$/$Cu_{224}$ center

The difference spectrum in Fig. 1(c), which was calculated from the spectra measured on the Ga-doped crystal, clearly

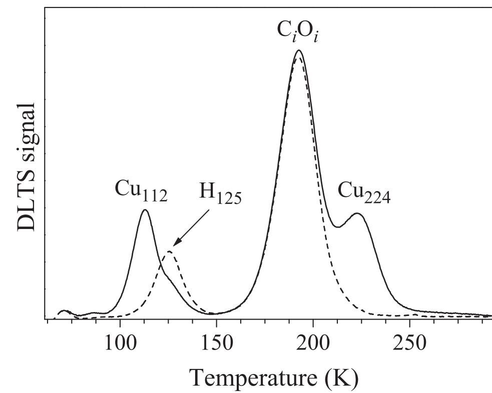


FIG. 2. DLTS spectra of the electron-irradiated Ga-doped crystal (no. 3) after 30 min annealing at 310 °C (dashed curve) and subsequent LT introduction of Cu at 350 K (solid curve). The spectra were taken from a depth of 1.8–2.5 $\mu$m.

demonstrates the presence of the $Cu_{112}$ level. Moreover, amplitudes of the $Cu_{112}$ and $Cu_{224}$ peaks are rather similar, suggesting that the two levels belong to the same center. This interpretation seems to contradict the DLTS spectra from the boron-doped material in Fig. 1(a). However, the amplitude of the underlying $V_2$ peak could be substantially lower after the LT-Cu treatment compared to the as-irradiated crystal, due to a passivation by hydrogen.[21] The dissociation rate for the GaH complex is ~200 times lower compared to BH,[22] therefore hydrogen penetration into the Ga-doped samples is negligible at 350 K as is also seen from the missing VOH peak in Fig. 1(b).

For a quantitative comparison of the $Cu_{112}$ and $Cu_{224}$ amplitudes, it is necessary to separate the $Cu_{112}$ and $V_2$ DLTS signals. Unfortunately, the LDLTS technique[19] fails to reliably resolve the components of the peak at 115 K in Fig. 1(b). Therefore, the as-irradiated samples were annealed at 310 °C for 30 min to remove the divacancies (Fig. 2, dashed curve). In the Ga-doped wafers this treatment introduces another level denoted as $H_{125}$. A similar annealing behavior was reported for Ga-doped electron-irradiated silicon by Khan *et al.*[23] The presence of the $H_{125}$ center does not interfere with the accurate measurements of the $Cu_{112}$ peak amplitude. The discussion on the (unknown) nature of the $H_{125}$ center is out of the scope of this paper.

The DLTS spectrum of the annealed Ga-doped sample after the LT-Cu treatment is shown in Fig. 2 by the solid line. The $Cu_{112}$ and $Cu_{224}$ levels are still formed in similar concentrations due to the introduction of Cu.

Depth profiles of the DL centers in this sample are shown in Fig. 3. The LT-Cu treatment changes the DL spectrum only in the layer of several micrometers below the surface. The concentrations of the $Cu_{112}$ and $Cu_{224}$ levels coincide within the error bar of ~10%.

In the boron-doped crystals the 310 °C annealing also removes divacancies and introduces the boron-related center with the DLTS peak at 146 K[24] (not shown). The subsequent LT-Cu treatment introduces both the $Cu_{112}$ and $Cu_{224}$ levels, and the $Cu_{112}$ concentration can be accurately measured. However, the $Cu_{224}$ signal strongly overlaps with the DLTS peak at 235 K. The latter peak is formed due to hydrogenation

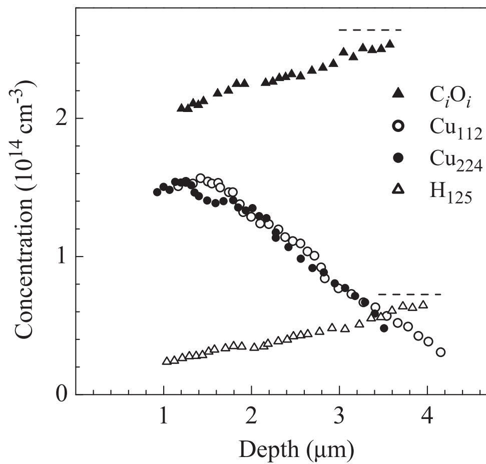


FIG. 3. Depth profiles of deep levels in the electron-irradiated Ga-doped crystal (no. 3) after the 30 min annealing at 310 °C and subsequent introduction of Cu at 350 K. The horizontal dashed lines indicate the $C_iO_i$ and $H_{125}$ concentrations before the LT-Cu treatment. Irradiation dose $\Phi = 3 \times 10^{15}$ cm$^{-2}$.

of the boron-related radiation defect which is present in as-irradiated FZ grown wafers and in the Cz-grown crystals after annealing above ∼200 °C.[16] Although the $Cu_{224}$ and $H_{235}$ signals can be easily separated by the LDLTS technique, the uncertainty of the $Cu_{224}$ concentration is larger in this case. Therefore, the identity of the $Cu_{112}$ and $Cu_{224}$ concentrations in the near-surface region of the boron-doped crystals, where the $H_{235}$ peak dominates the spectrum, can be confirmed with an accuracy of only ∼20%.

A close correspondence between the $Cu_{112}$ and $Cu_{224}$ concentrations is observed in all our samples for all preparation conditions (annealing at different temperatures before and after the introduction of copper, variations of the LT-Cu treatment, etc.). Thus, we infer that these two levels belong to the same defect.

It is seen also in Fig. 3 that the $C_iO_i$ and $H_{125}$ concentrations exhibit a noticeable decrease toward the surface after LT-Cu treatment. This confirms the earlier observation[8] that the $C_iO_i$ level disappears due to interaction with copper.

### C. $Cu_{112}$/$Cu_{224}$ precursor

The term "precursor" is used here to label the radiation defect in copper-free crystals which is involved in formation of the Cu-related defect. As seen from Fig. 3, the introduction rate for the $Cu_{112}$/$Cu_{224}$ precursor is not less than 0.05 cm$^{-1}$. Hence, the precursor should be one of the most abundant radiation defects.

Another characteristic of the precursor is the thermal stability. Therefore, the irradiated samples were annealed at different temperatures before the LT-Cu treatment. As shown in the previous section, the annealing at 310 °C results in no significant variation of the $Cu_{112}$/$Cu_{224}$ concentration [cf. Figs. 1(b) and 2, taking into account that the $C_iO_i$ center is stable at this temperature]. This result excludes divacancies and other defects which anneal out below ∼300 °C. The annealing at 340 °C for 30 min is found to reduce the $Cu_{112}$/$Cu_{224}$ concentration by a factor of 5 to 8 (in different crystals). If the annealing temperature is increased up to 365 °C, no $Cu_{112}$/$Cu_{224}$ centers are detected after the LT-Cu treatment. These data are in good agreement with the thermal stability of the A center (VO complex).[25]

In addition, our data totally rule out the $C_iO_i$ pair as a possible precursor of the $Cu_{112}$/$Cu_{224}$ center since the annealing at 365 °C reduces the $C_iO_i$ concentration only by ∼25%. The same conclusion has been drawn earlier based on the analysis of the DL depth profiles after the LT-Cu treatment[9] and is reconfirmed by the data in Fig. 3 where the decrement of the $C_iO_i$ concentration is about three times lower than the amount of the $Cu_{112}$/$Cu_{224}$ defects formed at around 1.5 $\mu$m depth. The other carbon-related defect, the $C_iC_s$ pair, is not considered as a possible precursor as its introduction rate is always low in oxygen-rich Cz-grown wafers.

Several boron-related radiation defects anneal out at 300–400 °C (Refs. 16,24,26) (Ga-doped material is less studied[23]). However, in the case of Cz-Si, all these defects are formed only upon recovery of the $B_iO_i$ pair at 150–200 °C, while the $Cu_{112}$/$Cu_{224}$ precursor already exists in the as-irradiated wafers. Besides, it is quite unlikely that the group III atom is a constituent of the $Cu_{112}$/$Cu_{224}$ center since the same DL activation energies are measured in B- and Ga-doped crystals.

Hence, we infer that the VO complex serves as a precursor of the $Cu_{112}$/$Cu_{224}$ center which we will label CuVO in the following.

### D. Thermal stability of the Cu-related centers

The LT-Cu treated samples are not suitable for the annealing experiments because the Cu-related defects are localized only in the near-surface layer (see Fig. 3). This layer will be strongly affected by hydrogen, which is introduced during chemical etching (see Sec. II B). Therefore, another approach of copper doping will be applied.

Contrary to the LT-Cu treatment the copper interaction with radiation defects can be generated by irradiation of Cu-contaminated samples.[6,9,27] These samples show a homogeneous distribution of the Cu-related defects and are convenient for annealing experiments.

The initial wafers were contaminated with copper at 750 °C (HT-Cu diffusion, see Sec. II B) and then irradiated with electrons at room temperature. The DL spectrum of such samples (not shown, see also Ref. 9) exhibits the same three Cu-related levels, $Cu_{112}$, $Cu_{224}$, and $Cu_{275}$, which are observed after the LT-Cu treatment (Fig. 1). The most significant quantitative difference is a relatively higher amplitude of the $Cu_{275}$ peak. The postirradiation anneals of the HT-Cu samples reveal that the $Cu_{275}$ level has a low thermal stability and is recovered by the 30 min treatment at 360 K. This fact explains the above-mentioned difference as the $Cu_{275}$ center undergoes a partial annealing during the LT-Cu treatment. A detailed discussion on the nature and the properties of the $Cu_{275}$ level is out of the scope of this paper.

The $Cu_{112}$ and $Cu_{224}$ levels of the CuVO center remain unchanged after annealing for 40 min at $\leqslant$250°C. Increasing the annealing temperature up to 300 °C, generates in addition $Cu_{103}$ and $Cu_{220}$ levels. While the $Cu_{103}$ level is clearly resolved in the DLTS spectrum, the $Cu_{220}$ level strongly overlaps with the $Cu_{224}$ signal and shows up only as a

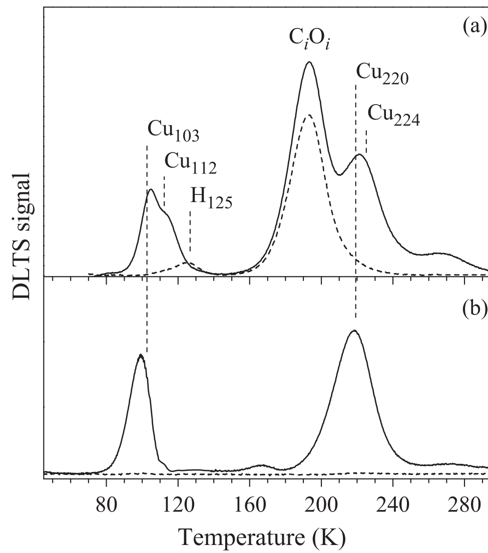


FIG. 4. DLTS spectra of a clean (dashed curves) and Cu-contaminated samples (solid curves) after electron irradiation and subsequent annealing at (a) 300 °C and (b) 400 °C for 40 min. (a) Crystal no. 3, $[Cu] = 5 \times 10^{14}$ cm$^{-3}$ (before the irradiation), $\Phi = 7 \times 10^{14}$ cm$^{-2}$; (b) crystal no. 5, $[Cu] = 8 \times 10^{14}$ cm$^{-3}$, $\Phi = 7 \times 10^{15}$ cm$^{-2}$. The peaks in (b) are shifted to lower temperatures due to stronger electric field in this higher doped crystal. The measurement conditions excluded signals close to the surface.

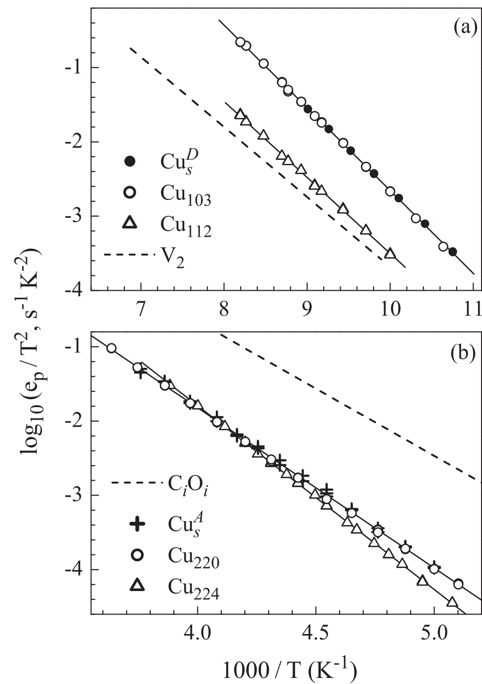


FIG. 5. Arrhenius plots of the hole emission rates from the denoted DL centers.

shift of the high-temperature peak to a lower temperature [Fig. 4(a)]. Further increase of the annealing temperature results in the total disappearance of the CuVO levels, while the behavior of the $Cu_{103}$ and $Cu_{220}$ levels varies in different crystals. In some cases, these levels also disappear and no significant difference remains between the DLTS spectra of clean and Cu-contaminated samples. In other crystals, the $Cu_{103}$ and $Cu_{220}$ levels survive the 400 °C annealing at which all normal radiation defects disappear from the DLTS spectrum [Fig. 4(b)]. The reasons for such a behavior could be the difference in the amount of Cu and radiation defects in the samples.

A feature repeatedly observed in different crystals is an increase of the DLTS peak at ∼190 K by 20–40% after the 300 °C annealing of the Cu-contaminated samples [Fig. 4(a)]. We relate this increase with the growing $C_iO_i$ concentration as no indications were found that another center contributes to the peak. At the moment, there is no plausible explanation of the phenomenon.

### E. $Cu_{103}/Cu_{220}$ center

The similarity of the $Cu_{103}$ and $Cu_{220}$ peak amplitudes in Fig. 4(b) suggests that the two levels belong to the same center. Thorough calculations, which also take into account the dependence of the $Cu_{103}$ peak amplitude on the electric field,[28] show that concentrations of the $Cu_{103}$ and $Cu_{220}$ levels are equal within the error bar of a few percent.

After the anneal at intermediate temperatures in the range 300–400 °C, a quantitative analysis of the concentrations is more difficult because the $Cu_{220}$ and $Cu_{224}$ peaks are so close that their contributions to the DLTS signal cannot be separated. Fortunately, the $Cu_{103}$ and $Cu_{112}$ levels can be easily resolved by LDLTS. We calculate $[Cu_{220}]$ by subtracting $[Cu_{112}]$ (equal to $[Cu_{224}]$) from the measured sum ($[Cu_{220}] + [Cu_{224}]$) (the brackets stand for the concentration values). In all cases the concentrations of the $Cu_{103}$ and $Cu_{220}$ levels are equal within an accuracy of 10%. The sum concentration of the CuVO and $Cu_{103}/Cu_{220}$ centers remains roughly constant due to anneals in the range 250–350 °C suggesting that the CuVO center transforms to the $Cu_{103}/Cu_{220}$ one.

### F. Arrhenius plots

Activation energies for the hole emissions from the observed DL centers have been measured using the LDLTS technique. The capacitance transients were recorded at several stabilized temperatures and then the emission rates were extracted for each deep level contributing to the transients.[19] The results are presented in Fig. 5 and summarized in Table II.

As seen in Fig. 5(a), the hole emission rates for $Cu_{112}$ and divacancy donor levels differ by a factor of ∼2 in the temperature range of interest. This separation is close to the limit where two levels can be resolved by LDLTS.[19] Therefore, the parameters of these levels were determined on samples where only one of the levels was present (the clean as-irradiated wafers and the Cu-contaminated crystals annealed at 310 °C, respectively). For the $Cu_{224}$ and $Cu_{220}$ levels we used the irradiated Cu-contaminated samples, which were annealed at ⩽100 °C or ⩾300 °C, respectively.

The $Cu_{224}$ level seems to be identical to the $E_v + 0.52$ eV level which was reported in the literature to form under similar conditions.[8] At the lowest temperature (∼190 K), the difference between the emission rates measured in Ref. 8 and in this work corresponds to a shift of only 0.3 K in the DLTS peak position. At ∼225 K (the highest peak temperature in Ref. 8),

TABLE II. Summary of defect properties: Level, activation energy $E_A$, apparent hole capture cross section $\sigma_p$, and level assignment.

| Level | $E_A$ (meV)[a] | $\sigma_p$ (cm$^{-2}$)[b] | Assignment |
|---|---|---|---|
| $Cu_{112}$ | $204 \pm 3$ | $1.6 \times 10^{-15}$ | CuVO $^{(0/+)}$ |
| $Cu_{224}$ | $494 \pm 4$ | $3.8 \times 10^{-14}$ | CuVO $^{(-/0)}$ |
| $Cu_{103}$ | $225 \pm 2$ | $1.2 \times 10^{-13}$ | $Cu_s^*$ $^{(0/+)}$ |
| $Cu_{220}$ | $432 \pm 2$ | $2.0 \times 10^{-15}$ | $Cu_s^*$ $^{(-/0)}$ |
| $Cu_s^D$ | $221 \pm 2$ | $7.3 \times 10^{-14}$ | $Cu_s$ $^{(0/+)}$ |
| $Cu_s^A$ | $430 \pm 3$ | $1.8 \times 10^{-15}$ | $Cu_s$ $^{(-/0)}$ |
| $V_2^D$ | $188 \pm 3$ | $1.6 \times 10^{-16}$ | $V_2$ $^{(0/+)}$ |
| $C_iO_i^D$ | $362 \pm 3$ | $1.2 \times 10^{-15}$ | $C_iO_i$ $^{(0/+)}$ |

[a]The shown uncertainty includes both the point scattering and the sample-to-sample variations.
[b]Calculated from the Arrhenius plot for emission rates with $\upsilon_{th}N_v = 3.3 \times 10^{21}$ T$^2$ cm$^{-2}$ s$^{-1}$.

such a shift increases up to ~2.5 K that can be attributed to a stronger impact on the position of the $E_v + 0.52$ eV peak from the overlapping $C_iO_i$ signal. (For the LDLTS technique used in this work the presence of the $C_iO_i$ peak is insignificant.)

All $Cu_{xxx}$ levels presented in Table II are close to a pair of the deep levels repeatedly observed in the (nonirradiated) Si crystals which were either Cu diffused at $T \gtrsim 900$ °C or doped with Cu from the melt during crystal growth. These levels are commonly believed to originate from the isolated substitutional copper atom $Cu_s$. Although the activation energies reported in the literature show some scattering, the pattern of levels is the same in all reports.[14,29–31] In the lower half of the band gap, the donor $Cu_s^D$ and acceptor $Cu_s^A$ levels are located at $E_v$+(0.21–0.23) and $E_v$+(0.42–0.48) eV, respectively. For an accurate comparison, the $Cu_s$ levels have been measured in the present work on the same setup and under similar conditions as those used for the irradiated samples. The wafer used for this purpose was doped with copper and boron during growth (for details, see Ref. 31). The results are also presented in Fig. 5 and Table II.

The Arrhenius signatures for the $Cu_{220}$ and $Cu_s^A$ levels are practically identical. As for the $Cu_{103}$ and $Cu_s^D$ levels, their confident intervals are just contiguous in Table II. It can be noted that the two low-temperature points for the $Cu_{103}$ level drop below the line, which fits the $Cu_s^D$ data only in Fig. 5(a). On the other hand, the $Cu_s^D$ Arrhenius plot in our chemically etched samples can be systematically disturbed by the unresolved overlapping level.[31] Thus, the experimental data are not sufficient to show the different properties of the $Cu_{103}$/$Cu_{220}$ center and substitutional copper. However, for the sake of generality, the center with the $Cu_{103}$/$Cu_{220}$ levels is referred to as $Cu_s^*$ in Table II. Additional reasons to distinguish $Cu_s^*$ from $Cu_s$ will be given below.

### G. Structure of the CuVO complex

The CuVO complex is formed during the LT-Cu treatment by $Cu_i^+$ diffusion to the neutral VO center. The same mechanism occurs during irradiation of the HT-Cu diffused crystals as copper is mobile at room temperatures. A simple estimate shows that within several seconds after formation the VO center can interact with the diffusing $Cu_i^+$ species. An alternative mechanism of the CuVO complex formation by interaction of the vacancy with a preexisting $Cu_iO_i$ pair seems to be less probable. The experimentally[32] and theoretically[33] determined binding energies for the $Cu_iO_i$ pair are too low ($\leqslant$0.3 eV) to bind a dominant part of the copper in the sample. In addition, the $Cu_iO_i$ pairs have to compete for vacancies with interstitial oxygen which concentration is more than four orders of magnitude higher in the Cz-grown crystals.

Several publications discuss the interactions of copper with radiation defects from the theoretical point of view. For the purpose of the present work, it is important that the reaction of $Cu_i$ with a preexisting vacancy leads to the formation of $Cu_s$ at a gain in energy of 2.7–2.8 eV depending on the theory level.[34] The $Cu_i$ interactions with divacancies or self-interstitials are also exothermal with energy gains of 2.5 and 1.4 eV, respectively.

The reaction of $Cu_i$ with the VO complex has been discussed by two groups.[33,35] The molecular-dynamics simulations show that $Cu_i$ displaces oxygen from the vacancy and becomes $Cu_s$, while $O_i$ occupies the adjacent Si-Si bond.[33] The formation of this $\{Cu_s,O_i\}$ complex releases about 1.7 eV. Unfortunately, the deep levels related to the complex were not calculated by the authors.

The analysis in Hartree-Fock approximation[35] gives similar energy gains of 1.5–1.6 eV for the formation of two possible configurations of the CuVO complex: Cu either occupies the substitutional site or stays interstitial. Based on the evaluated energy barriers for different reactions, formation of the $Cu_iVO$ center seems to be preferable.[6,35] In the $Cu_iVO$ complex the original electronic structure of the VO center is basically preserved and the electrical activity can be derived by perturbation theory. The acceptor level of the VO center was calculated to shift to the midgap position.[35] This result served as an additional argument to ascribe the experimentally observed $E_c - 0.60$ eV level to the $Cu_iVO$ complex.[6]

In the present work a strong resemblance between the level patterns of the CuVO and $Cu_s$ centers is observed (see Table II). Therefore, we propose that the CuVO center has the structure of the $\{Cu_s,O_i\}$ complex predicted in Ref. 33. Taking into account that the $Cu_s$ double acceptor level is located at $E_c$−(0.16–0.17) eV,[14,29] the $E_c - 0.17$ eV level (assigned to a $CuV_2$ complex)[6] would perfectly fit to the CuVO level structure in close analogy to the $Cu_s$ levels. It is noteworthy that the $E_c - 0.17$ eV center anneals out above 300 °C (Ref. 6) in accordance with the behavior of the $Cu_{112}$ and $Cu_{224}$ levels. At the same time, the $E_c - 0.60$ eV level, which was assigned to the $Cu_iVO$ complex,[6] cannot be correlated with the $Cu_{224}$ level. Although these two levels are close in the band gap ($E_c - 0.60$ and $E_v + 0.49$ eV), their Arrhenius signatures are quite different.

The annealing at $\geqslant$300 °C results in a transformation of the $\{Cu_s,O_i\}$ complex into a $Cu_s^*$ center with levels which are virtually identical to those of $Cu_s$ (Table II). The transformation can be visualized as a dissociation of the $\{Cu_s,O_i\}$ complex. The binding energy between $Cu_s$ and $O_i$ was calculated to be as low as 0.4–0.5 eV,[33] but the $O_i$ diffusivity is too low at these temperatures to account for the dissociation process. The mean time for an isolated $O_i$ atom to jump to one of the adjacent Si-Si bonds is several hours at 400 °C and years at 300 °C.[36] It could be assumed

that the diffusion barrier for $O_i$ is lowered in the vicinity of $Cu_s$. The calculations show that nearly no lattice distortion occurs around $Cu_s$.[33] Therefore, the barrier lowering has to be limited to few lattice parameters, at which distance the oxygen atom is expected to get stuck. This is the reason to denote the $Cu_{103}/Cu_{220}$ center as $Cu_s^*$ to distinguish it from the isolated $Cu_s$ center.

Our experimental data show no indication for any intermediate levels between $Cu_{103}$ and $Cu_{112}$. Most probably, this means that even a single $O_i$ jump to the next coordination shell is enough to reduce the effect of the nearby oxygen on the $Cu_s$ energy levels below the practical limit for electrical measurements.

Note that the "near-substitutional" Cu was found in Cu-implanted silicon by the emission channeling technique.[37] This center, which anneals out in a wide temperature range from 250 to 600 °C, seems to be irrelevant for the discussion on $Cu_s^*$ since it was observed in oxygen-lean crystals where the implanted Cu concentration exceeds that of oxygen by two to three orders of magnitude.

## IV. CONCLUSION

We have detected Cu-related levels in the lower half of the band gap which are formed either due to the Cu introduction into irradiated Si at temperatures below 100 °C or as a result of the irradiation of Cu-contaminated wafers. In both cases the reactions are determined by diffusion of the $Cu_i$ species to radiation defects.

Two of the most prominent levels formed below 100 °C, $Cu_{112}$ and $Cu_{224}$, always appear in the same concentrations and are attributed to the same center. The high introduction rate of this center can be explained if its precursor is one of the dominant radiation defects in the sample. Based on the DL depth profiles after the low-temperature copper introduction and the thermal stability of radiation defects, the precursor is identified as the well-known VO center. The $Cu_{112}$ and $Cu_{224}$ levels of the CuVO center differ from the donor and acceptor levels of substitutional copper $Cu_s$ by only 0.02 and 0.06 eV, respectively. This similarity supports the $\{Cu_s, O_i\}$ model predicted in the literature to be a result of the reaction between $Cu_i$ and the VO center.

The CuVO center anneals at $\geqslant 300$°C and transforms into a defect where the two levels are practically coincident with the donor and acceptor levels of the substitutional copper atom. This transformation appears to proceed via emission of the $O_i$ atom from the defect. However, the well-known oxygen mobility in this temperature range locates the emitted $O_i$ atom within a few lattice parameters from $Cu_s$. Calculations are required to estimate how the oxygen atom located in the closest coordination shells affects the $Cu_s$ levels.

## ACKNOWLEDGMENTS

The authors are indebted to Professor A. Mesli and Dr. P. Wagner for supplying the Ga-doped samples and to Dr. Vl. Kolkovsky for his help with the LDLTS measurements. N.Y. acknowledges the support by an Erasmus Mundus Scholarship (EM ECW-L04).

*nay@iptm.ru

[1] E. R. Weber, Appl. Phys. A **30**, 1 (1983).
[2] A. A. Istratov and E. R. Weber, Appl. Phys. A **66**, 123 (1998).
[3] A. A. Istratov and E. R. Weber, J. Electrochem. Soc. **149**, G21 (2002).
[4] S. Knack, Mater. Sci. Semicond. Process. **7**, 125 (2004).
[5] B. G. Svensson, M. O. Aboelfotoh, and J. L. Lindström, Phys. Rev. Lett. **66**, 3028 (1991).
[6] V. P. Markevich, A. R. Peaker, I. F. Medvedeva, V. Gusakov, L. I. Murin, and B. G. Svensson, Solid State Phenom. **131–133**, 363 (2008).
[7] S. J. Pearton and A. J. Tavendale, J. Appl. Phys. **54**, 1375 (1983).
[8] M. O. Aboelfotoh and B. G. Svensson, Phys. Rev. B **52**, 2522 (1995).
[9] N. Yarykin and J. Weber, Semiconductors **44**, 983 (2010).
[10] A. A. Istratov, C. Flink, H. Hieslmair, E. R. Weber, and T. Heiser, Phys. Rev. Lett. **81**, 1243 (1998).
[11] T. Prescha and J. Weber, Mater. Sci. Forum **83–87**, 167 (1992).
[12] A. Mesli and T. Heiser, Phys. Rev. B **45**, 11632 (1992).
[13] K. Graff and H. Pieper, in *Semiconductor Silicon*, edited by H. R. Huff and R. J. Kriegler (The Electrochemical Society, Pennington, New Jersey, 1981), p. 331.
[14] S. D. Brotherton, J. R. Ayres, A. A. Gill, H. W. van Kesteren, and F. J. A. M. Greidanus, J. Appl. Phys. **62**, 1826 (1987).
[15] O. V. Feklisova, N. Yarykin, E. B. Yakimov, and J. Weber, Physica B **308–310**, 210 (2001).
[16] N. Yarykin, O. V. Feklisova, and J. Weber, Phys. Rev. B **69**, 045201 (2004).
[17] L. C. Kimerling, J. Appl. Phys. **45**, 1839 (1974).
[18] D. Stievenard and D. Vuillaume, J. Appl. Phys. **60**, 973 (1986).
[19] L. Dobaczewski, A. R. Peaker, and K. Bonde Nielsen, J. Appl. Phys. **96**, 4689 (2004).
[20] The same peak was denoted as $Cu_{220}$ in Ref. 9. We have changed the notation for the reason which is made clear later in the text.
[21] O. V. Feklisova, E. B. Yakimov, N. Yarykin, and J. Weber, Semiconductors **35**, 1355 (2001).
[22] T. Zundel and J. Weber, Phys. Rev. B **39**, 13549 (1989).
[23] A. Khan, M. Yamaguchi, Y. Ohshita, N. Dharmarasu, K. Araki, T. Abe, H. Itoh, T. Ohshima, M. Imaizumi, and S. Matsuda, J. Appl. Phys. **90**, 1170 (2001).
[24] P. M. Mooney, L. J. Cheng, M. Süli, J. D. Gerson, and J. W. Corbett, Phys. Rev. B **15**, 3836 (1977).
[25] J. W. Corbett, G. D. Watkins, R. M. Chrenko, and R. S. McDonald, Phys. Rev. **121**, 1015 (1961).
[26] L. C. Kimerling, M. T. Asom, J. L. Benton, P. J. Drevinsky, and C. E. Caefer, Mater. Sci. Forum **38–41**, 141 (1989).
[27] S. Tamulevicius, B. G. Svensson, M. O. Aboelfotoh, and A. Hallén, J. Appl. Phys. **71**, 4212 (1992).

[28] N. Yarykin and J. Weber (unpublished). (The rate of hole emission from the $Cu_s$ donor level under electric field is shown to be described by the phonon-assisted tunneling model.)
[29] H. Lemke, Phys. Status Solidi A **95**, 665 (1986) (in German).
[30] H. Lemke, Mater. Sci. Forum **196–201**, 683 (1995).
[31] S. Knack, J. Weber, H. Lemke, and H. Riemann, Phys. Rev. B **65**, 165203 (2002).
[32] A. Mesli, T. Heiser, and E. Mulheim, Mater. Sci. Eng. B **25**, 141 (1994).
[33] D. West, S. K. Estreicher, S. Knack, and J. Weber, Phys. Rev. B **68**, 035210 (2003).
[34] S. K. Estreicher, Phys. Rev. B **60**, 5375 (1999); S. K. Estreicher, D. West, J. M. Pruneda, S. Knack, and J. Weber, Mater. Res. Soc. Symp. Proc. **719**, F13.9.1 (2002).
[35] V. E. Gusakov, in *Proceedings of the International Workshop on Radiation Physics of Solid State*, edited by G. G. Bondarenko (Moscow, 2008), p. 642 (in Russian).
[36] J. W. Corbett, R. S. McDonald, and G. D. Watkins, J. Phys. Chem. Solids **25**, 873 (1964); R. C. Newman, J. Phys.: Condens. Matter **12**, R335 (2000).
[37] U. Wahl, A. Vantomme, G. Langouche, J. G. Correia, and ISOLDE Collaboration, Phys. Rev. Lett. **84**, 1495 (2000).